

EXPLAINING OSCILLATORY BEHAVIOR IN CONVECTION-DIFFUSION DISCRETIZATION

CONSTANTIN BACUTA

ABSTRACT. For a model convection-diffusion problem, we address the presence of oscillatory discrete solutions, and study difficulties in recovering standard approximation results for its solution. We justify the presence of non-physical oscillations and propose ways to eliminate oscillations. A new approach for error analysis that requires establishing optimal discrete infinity error as a first step is introduced and justified. We emphasize that the discretization of two dimensional convection dominated problems benefit from the efficient discretization of the corresponding one dimensional problem along each stream line. Our results are useful in building new and robust discretizations for multi-dimensional convection dominated problems.

1. INTRODUCTION

We consider the model of a singularly perturbed convection diffusion problem: Given data $f \in L^2(\Omega)$, find $u \in H_0^1(\Omega)$ such that

$$(1.1) \quad \begin{cases} -\varepsilon \Delta u + \mathbf{b} \cdot \nabla u = f & \text{in } \Omega, \\ u = 0 & \text{on } \partial\Omega, \end{cases}$$

for a positive constant ε and a bounded domain $\Omega \subset \mathbb{R}^d$. We assume that $\varepsilon \ll 1$, and that the vector \mathbf{b} is chosen such that a unique solution exists.

For the one dimensional case, we further assume that f is continuous on $[0, 1]$, $\mathbf{b} = 1$ and look for $u = u(x)$ such that

$$(1.2) \quad \begin{cases} -\varepsilon u''(x) + u'(x) = f(x), & 0 < x < 1 \\ u(0) = 0, \quad u(1) = 0. \end{cases}$$

The model problem (1.1) arises when solving heat transfer problems in thin domains, as well as when using small step sizes in implicit time discretizations of parabolic convection diffusion type problems, see [21]. The solutions to the model problem (1.1) is characterized by boundary layers, see e.g., [19, 22, 24, 27]. Approximating such solutions poses numerical challenges due to the ε -dependence of the stability constants and of the error estimates. In applications, the model problem (1.1) could be coupled with

2020 *Mathematics Subject Classification.* 80M10, 76M10, 65F, 65H10, 65N06, 65N12, 65N22, 65N30, 74S05, 76R10, 76R10.

Key words and phrases. non-oscillatory discretization, bubble upwinding Petrov-Galerkin, convection dominated problem, singularly perturbed problems.

a more complex system of equations such as the Navier-Stokes equations through the convection vector \mathbf{b} .

The variational formulation of (1.1) is: Find $u \in Q := H_0^1(\Omega)$ such that

$$(1.3) \quad b(v, u) := (\varepsilon \nabla u, \nabla v) + (\mathbf{b} \cdot \nabla u, v) = (f, v) \quad \text{for all } v \in V := H_0^1(\Omega).$$

Throughout this paper, (\cdot, \cdot) denotes the scalar or vector L^2 inner product.

For the discretization of (1.3), we assume that $\mathcal{M}_h \subset Q$ and $V_h \subset V$ are finite element spaces that are compatible spaces, in the sense that $b(\cdot, \cdot)$ satisfies a discrete inf-sup condition on $V_h \times \mathcal{M}_h$.

A general Petrov-Galerkin (PG) discretization of (1.3) with $\dim(V_h) = \dim(\mathcal{M}_h)$ is: Find $u_h \in \mathcal{M}_h$ such that

$$(1.4) \quad b(v_h, u_h) = (f, v_h) \quad \text{for all } v_h \in V_h.$$

The Saddle Point Least Square (SPLS) approach uses an auxiliary variable that represents the residual of the variational formulation (1.4) on the test space. This brings in another simple equation involving the residual variable. The method leads to a square symmetric saddle point system. The SPLS discretization of (1.3) is: Find $(w_h, u_h) \in V_h \times \mathcal{M}_h$ such that

$$(1.5) \quad \begin{aligned} a_0(w_h, v_h) + b(v_h, u_h) &= (f, v_h) && \text{for all } v_h \in V_h, \\ b(w_h, q_h) &= 0 && \text{for all } q_h \in \mathcal{M}_h, \end{aligned}$$

where $a_0(u, v) := (\nabla u, \nabla v)$. The component u_h of (w_h, u_h) is the *SPLS discrete solution* of (1.3). We can view the PG discretization as a particular case of SPLS discretization for which $w_h = 0$ in (1.5).

The Galerkin method applied to (1.4), with $\mathcal{M}_h = V_h$ being a standard finite element space of continuous piecewise polynomials on uniform meshes, leads to numerical pollution which translates into non-physical oscillation of the numerical solution, unless $h \approx \varepsilon$ or $h < \varepsilon$. Even if the mesh is adapted in the boundary layers regions, see e.g. [5, 17], an SPLS discretization such as the $P^1 - P^2$ discretization can still produce non-physical oscillations.

The goal of the paper is to analyze the presence of non-physical oscillations, to propose ways to avoid such oscillations, and to propose a new approach for establishing approximation errors for convection dominated problems.

The rest of the paper is organized as follows. Section 2 contains a review of the main results on the optimal trial norms for the convection diffusion problem. The Standard Linear (SL), the Saddle Point Least Square (SPLS) discretization errors and non-physical oscillations analyses are presented in Section 3. The one dimensional Upwinding Petrov-Galerkin (UPG) method emphasizing on non-oscillatory behavior of the discrete solution is summarized in Section 4. In Section 5, for the one dimensional case, we motivate the importance of recovering the exact solution at the nodes and the advantages of discrete infinity norm approximation towards eliminating non-physical oscillations. In Section 6, for a two dimensional case, we review the quadratic bubble UPG approximation properties and explain the oscillations along the parabolic boundary layer. We summarize our findings in Section 7.

2. OPTIMAL TRIAL NORM FOR THE CONVECTION DIFFUSION PROBLEM

We consider the variational formulation (1.3) with $V = Q = H_0^1(\Omega)$ and consider different norms on the test and trial spaces. On the test space $V := H_0^1(\Omega)$, we consider the norm induced by

$$a_0(u, v) := (\nabla u, \nabla v).$$

From the stability point of view, to define the optimal norm on Q , we represent the *antisymmetric part* of the bilinear form $b(\cdot, \cdot)$ in the $a_0(\cdot, \cdot)$ inner product as follows. Let $T : Q \rightarrow V$ be the representation operator defined by

$$a_0(Tu, v) = (b \cdot \nabla u, v), \quad \text{for all } v \in V.$$

It is easy to check that

$$|Tu| = \|b \cdot \nabla u\|_{H^{-1}(\Omega)} \leq \|b\| \|u\|_{L^2(\Omega)}.$$

For the one dimensional case and $\mathbf{b} = 1$, we have

$$a_0(Tu, q) = (u', q), \quad \text{for all } q \in Q.$$

By solving the corresponding differential equation, one can find that

$$(2.1) \quad Tu = x\bar{u} - \int_0^x u(s) ds,$$

and

$$(2.2) \quad |Tu|^2 = \int_0^1 |u(s) - \bar{u}|^2 ds = \|u - \bar{u}\|^2 = \|u\|^2 - \bar{u}^2 \leq \|u\|^2.$$

Throughout the paper, for $v \in L^2(0, 1)$, we denote $\bar{v} := \int_0^1 v(x) dx$.

The continuous *optimal trial norm* on Q is defined by

$$\|u\|_* := \sup_{v \in V} \frac{b(v, u)}{|v|} = \sup_{v \in V} \frac{\varepsilon a_0(u, v) + a_0(Tu, v)}{|v|}.$$

Using the Riesz representation theorem and $a_0(Tu, u) = 0$, we obtain

$$(2.3) \quad \|u\|_*^2 = \varepsilon^2 |u|^2 + |Tu|^2.$$

For the one dimensional case, from (2.2), we get

$$(2.4) \quad \|u\|_*^2 = \varepsilon^2 |u|^2 + \|u\|^2 - \bar{u}^2.$$

Next, we assume that $V_h \subset V = H_0^1(\Omega)$ and $\mathcal{M}_h \subset Q = H_0^1(\Omega)$ are discrete finite element spaces and that $\mathcal{M}_h \subset V_h$. To describe the *discrete optimal norm* on \mathcal{M}_h , we will need the standard elliptic projection $P_h : Q \rightarrow V_h$ defined by

$$a_0(P_h u, v_h) = a_0(u, v_h), \quad \text{for all } v_h \in V_h.$$

The optimal trial norm on \mathcal{M}_h is

$$(2.5) \quad \|u_h\|_{*,h} := \sup_{v_h \in V_h} \frac{b(v_h, u_h)}{|v_h|}.$$

As in the continuous case, see [12, 15], by denoting $|u|_{*,h} := |P_h Tu|$, we have

$$(2.6) \quad \|u_h\|_{*,h}^2 = \varepsilon^2 |u_h|^2 + |P_h Tu_h|^2 = \varepsilon^2 |u_h|^2 + |u_h|_{*,h}^2.$$

The advantage of using the optimal trial norm on Q and \mathcal{M}_h resides with the fact that both $\inf - \sup$ and $\sup - \sup$ constants at the continuous and discrete levels are equal to one. The following error estimate was proved in [15].

Theorem 2.1. *Let $\|\cdot\|_*$ and $\|\cdot\|_{*,h}$ be the norms on Q , and \mathcal{M}_h and assume:*

$$(2.7) \quad \|v\|_* \leq c_0 \|v\|_{*,h} \quad \text{for all } v \in Q.$$

Let u be the solution of (1.3) and let u_h be the unique solution of the problems (1.4) or (1.5). Then, the following error estimate holds:

$$(2.8) \quad \|u - u_h\|_{*,h} \leq c_0 \inf_{p_h \in \mathcal{M}_h} \|u - p_h\|_{*,h}.$$

2.1. Discrete optimal trial norm for the one dimensional case. We review a representation formula for $|\cdot|_{*,h}$ that was discussed in [5, 12].

For $V = Q = H_0^1(0, 1)$ we consider the standard inner product given by $a_0(u, v) = (u, v)_V = (u', v')$. We divide the interval $[0, 1]$ into n equal length subintervals using the nodes $0 = x_0 < x_1 < \cdots < x_n = 1$ and denote $h := x_j - x_{j-1}$, $j = 1, 2, \dots, n$. We define the corresponding finite element discrete space \mathcal{M}_h as the space of all *continuous piecewise linear functions* with respect to the given nodes, that are zero at $x = 0$ and $x = 1$.

Next, we let \mathcal{M}_h, V_h be the standard spaces of continuous piecewise linear functions

$$\mathcal{M}_h = V_h = \text{span}\{\varphi_1, \dots, \varphi_{n-1}\}.$$

In this case, the explicit formula for $|u|_{*,h} = |P_h Tu|$ is

$$(2.9) \quad |u|_{*,h}^2 := |P_h Tu|^2 = \frac{1}{n} \sum_{i=1}^n \left(\frac{1}{h} \int_{x_{i-1}}^{x_i} u(x) dx \right)^2 - \left(\int_0^1 u(x) dx \right)^2.$$

Remark 2.2. *Note that $|\cdot|_{*,h}$ is a seminorm on \mathcal{M}_h . For $n = 2m$ and $\omega_h := \varphi_1 + \varphi_3 + \cdots + \varphi_{2m-1}$, we have $|\omega_h|_{*,h} = 0$. The graph of ω_h has a “teeth saw” shape and can be highly oscillatory when $h = 1/n$ is small.*

3. THE SL AND SPLS DISCRETIZATIONS EXHIBIT NON-PHYSICAL OSCILLATIONS

In this section, for the one dimensional case, we focus on the Standard Linear (SL) discretization with $C^0 - P^1$ test and trial spaces, and on the SPLS discretization with $C^0 - P^1$ trial space and $C^0 - P^2$ test space. We explain the oscillatory behavior for both discretizations based on the error analysis in the optimal trial norms, and on the *closeness* between the discrete solution and the related transport problems.

For the finite element discretization, we use the following notation:

$$a_0(u, v) = \int_0^1 u'(x)v'(x) dx, \quad (f, v) = \int_0^1 f(x)v(x) dx, \text{ and}$$

$$b(v, u) = \varepsilon a_0(u, v) + (u', v) \text{ for all } u, v \in V := H_0^1(0, 1).$$

A variational formulation of (1.2) is: Find $u \in V := H_0^1(0, 1)$ such that

$$(3.1) \quad b(v, u) = (f, v), \text{ for all } v \in V = H_0^1(0, 1).$$

3.1. Standard discretization with $C^0 - P^1$ test and trial spaces. We divide the interval $[0, 1]$ into n equal length subintervals using the nodes $0 = x_0 < x_1 < \dots < x_n = 1$ and denote $h := x_j - x_{j-1}, j = 1, 2, \dots, n$. For the above uniform distributed notes on $[0, 1]$, we define the corresponding finite element discrete space \mathcal{M}_h as the subspace of $Q = H_0^1(0, 1)$, given by

$$\mathcal{M}_h = \{v_h \in Q \mid v_h \text{ is linear on each } [x_j, x_{j+1}]\},$$

i.e., \mathcal{M}_h is the space of all *continuous piecewise linear functions* with respect to the given nodes, that are zero at $x = 0$ and $x = 1$. We consider the nodal basis $\{\varphi_j\}_{j=1}^{n-1}$ with the standard defining property $\varphi_i(x_j) = \delta_{ij}$. We couple the above discrete trial space with the discrete test space $V_h = \mathcal{M}_h$. Thus, the standard $C^0 - P^1$ variational formulation of (3.1) is:

Find $u_h \in \mathcal{M}_h$ such that

$$(3.2) \quad b(v_h, u_h) = \varepsilon(u'_h, v'_h) + (u'_h, w_h) = (f, v_h), \text{ for all } v_h \in V_h.$$

In this case, according to Section 2, we have $\|u_h\|_{*,h}^2 = \varepsilon^2|u_h|^2 + |u_h|_{*,h}^2$, where $|\cdot|_{*,h}^2$ has the representation given in (2.9).

As a consequence of Theorem 2.1, we proved in [5] the following result.

Theorem 3.1. *If u is the solution of (3.1) and u_h is the solution of the linear discretization (3.2), then*

$$\|u - u_h\|_{*,h} \leq c_0 \inf_{v_h \in V_h} \|u - v_h\|_{*,h}, \text{ where}$$

$$c_0 = c(h, \varepsilon) = \sqrt{1 + \left(\frac{h}{\pi \varepsilon}\right)^2} \approx \frac{h}{\pi \varepsilon} \text{ if } \varepsilon \ll h.$$

Numerical tests performed for [5] show that, as $\varepsilon \ll h$, the linear finite element solution of (3.2) presents non-physical oscillations.

To understand the presence of such oscillations, we consider the reduced continuous and discrete corresponding problems. By letting $\varepsilon \rightarrow 0$ in (3.1), we obtain the *reduced continuous problem*:

Find $u \in H_0^1(0, 1)$ such that

$$(3.3) \quad (u', v) = (f, v), \text{ for all } v \in V.$$

The problem (3.3) has unique solution, if and only if $\int_0^1 f(x) dx = 0$. On the other hand, the corresponding Left to Right (*LR*) *transport* problem:

Find $w \in H^1(0, 1)$ such that

$$(3.4) \quad w'(x) = f(x) \text{ for all } x \in (0, 1), \text{ and } w(0) = 0,$$

has unique solution: $w(x) = \int_0^x f(s) ds$, regardless of the average of the function f .

Similarly, the other related Right to Left (*RL*) *transport* problem: Find $\theta \in H^1(0, 1)$ such that

$$(3.5) \quad \theta'(x) = f(x) \text{ for all } x \in (0, 1), \text{ and } \theta(1) = 0,$$

has unique solution: $\theta(x) = w(x) - \int_0^1 f(x) dx$.

By letting $\varepsilon \rightarrow 0$ in (3.2), we obtain the *reduced discrete problem*:
Find $U_h \in \mathcal{M}_h$ such that

$$(3.6) \quad (U'_h, v_h) = (f, v_h), \text{ for all } v_h \in V_h = \mathcal{M}_h.$$

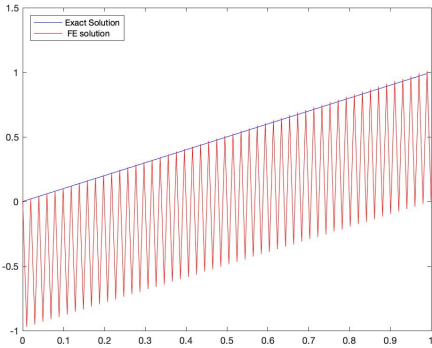


Fig.1: $f = 1, n = 99, \varepsilon = 10^{-6}$

u_h oscillate between x and $x - 1$ and very close to the solution U_h of (3.6)

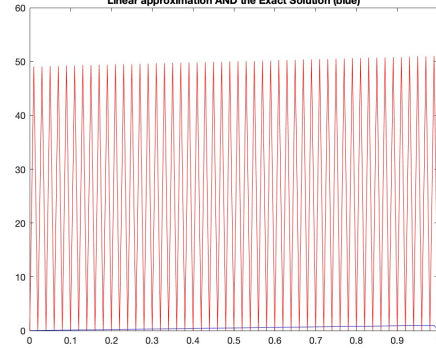


Fig.2: $f = 1, n = 100, \varepsilon = 10^{-6}$

$u_h \approx u + h^2/(2\varepsilon) \omega_h$. No solution for the reduced discrete problem (3.6).

If $\int_0^1 f(x) dx \neq 0$ and the number of subintervals $n = 1/h$ is odd, then the linear system associated with (3.6) has unique solution, see [5]. In this case, as $\varepsilon/h \rightarrow 0$, the finite element solution u_h of (3.2) is very close to the solution U_h of (3.6), and both solutions oscillate between the graph of the two transport problems RL and LR, i.e., w and θ , respectively.

If $\int_0^1 f(x) dx \neq 0$ and the number of subintervals n is even, the problem (3.6) might not have solution, but because of the week coercivity of the bilinear form $b(\cdot, \cdot)$ of (3.2), we have that (3.2) has an unique solution u_h . Numerically, as shown in Figure 2, we observed that for $\varepsilon/h \leq 10^{-4}$, at the nodes, u_h is very close to $u + h^2/(2\varepsilon) \omega_h$, where u is the solution of (3.1) and ω_h is the “teeth saw” function defined in Remark 2.2. Thus, at the nodes, we have that $u_h - u$ behaves like $h^2/(2\varepsilon) \omega_h$.

Regardless of the number of intervals, for $\int_0^1 f(x) dx \neq 0$ and for $\varepsilon < h$, for example $\varepsilon/h < 1/3$, we observe non-physical oscillations in the SL discrete solution.

If the *reduced discrete problem* does not have a solution, we can expect global non-physical oscillatory behavior of the discrete solution u_h of (3.2), and u_h could contain high frequency modes such as the “teeth saw” function.

If the *reduced discrete problem* does have a unique solution, but it does not correspond to the discretization of a reduced *continuous problem*, we can also expect global non-physical oscillations in the discrete solution.

Theorem 3.1 cannot control the discrete infinity error of the solution, hence it cannot predict the oscillatory behavior of the discrete solution.

3.2. Approximation for the SPLS discretization. A *saddle point least square* (SPLS) approach for solving (1.2) has been used before, for example in [5, 9, 17]. For $V = Q = H_0^1(0, 1)$, we look for finding $(w = 0, u) \in V \times Q$ such that

$$(3.7) \quad \begin{aligned} a_0(w, v) + b(v, u) &= (f, v) && \text{for all } v \in V, \\ b(w, q) &= 0 && \text{for all } q \in Q, \end{aligned}$$

where

$$b(v, u) = \varepsilon a_0(u, v) + (u', v) = \varepsilon (u', v') + (u', v).$$

Clearly, the component u of the solution $(w = 0, u)$ is the solution of (3.1). The advantage of considering the SPLS form is that its discretization leads to a symmetric linear system. Analyses for finite element test and trial spaces of various degree polynomials for (3.7) can be found in [17, 18].

For $P^1 - P^2$ discretization we follow the notation of [5]. We consider on $[0, 1]$ the uniformly distributed nodes $x_j = h j, j = 0, 1, \dots, n$, with $h = 1/n$ and define $\mathcal{M}_h = C^0 - P^1 := \text{span}\{\varphi_j\}_{j=1}^{n-1}$, with φ_j 's the standard linear nodal functions and $V_h = C^0 - P^2$ - the space of continuous piece-wise quadratic functions. The discrete version of (3.7) is:

Find $(w_h, u_h) \in V_h \times \mathcal{M}_h$ such that (1.5) is satisfied. The component u_h of (w_h, u_h) is the SPLS discretization of (1.2) or the SPLS solution of (1.5).

We note that the projection P_h defined in Section 2, is the projection on the space $V_h = C^0 - P^2$ of continuous piece-wise quadratic functions. For any piecewise linear function $u_h \in \mathcal{M}_h$, we have that

$$Tu_h = x\bar{u}_h - \int_0^x u_h(s) ds,$$

is a continuous piecewise quadratic function which is zero at the ends. Consequently, $Tu_h \in V_h$, and $P_h Tu_h = Tu_h$, and, according to (2.6) and (2.3), the optimal discrete norm on \mathcal{M}_h becomes

$$\|u_h\|_{*,h}^2 = \varepsilon^2 |u_h|^2 + |Tu_h|^2 = \|u_h\|_*^2.$$

Using the optimal norm on \mathcal{M}_h , a discrete inf - sup condition is satisfied, and the problem (1.5) has a unique solution. In addition, for the $P^1 - P^2$ SPLS discretization, we can consider the same norm given by

$$\|u\|_*^2 = \varepsilon^2 |u|^2 + \|u - \bar{u}\|^2 = \varepsilon^2 |u|^2 + \|u\|^2 - \bar{u}^2 = \|u\|_{*,h}^2$$

on both spaces Q and \mathcal{M}_h . Since (2.7) is satisfied with $c_0 = 1$, as a consequence of Theorem 2.1, we obtain:

Theorem 3.2. *If u is the solution of (3.1), and u_h is the SPLS solution of the $(P^1 - P^2)$ discretization (1.5), then*

$$\|u - u_h\|_* \leq \inf_{p_h \in \mathcal{M}_h} \|u - p_h\|_* \leq \|u - u_I\|_*,$$

where u_I is the interpolant of the exact solution on the h -uniformly distributed nodes on $[0, 1]$.

For $\int_0^1 f(x) dx = 0$, the $P^1 - P^2$ SPLS discretization improves on standard linear discretization of (3.1) from the error point of view, see e.g. [5, 17]. For $\int_0^1 f(x) dx \neq 0$ and $\varepsilon \ll h$, in spite of the optimal approximation result of Theorem 3.2, the SPLS solution u_h approximates a shift by a constant of the solution u of the continuous problem (3.7) or (3.1), and *local non-physical oscillations* still appear in the discrete solution u_h at the ends of the interval. More numerical experiments showing the oscillations are in [5].

3.3. The oscillatory behavior of $P^1 - P^2$ SPLS discretization. In this section, we justify why the $P^1 - P^2$ SPLS discretization fails to produce a good approximation for the solution of (3.1) for the case $\int_0^1 f(x) dx \neq 0$. In what follows, we use the notation and considerations of Section 3.2.

We consider the *reduced continuous problem* obtained from (3.7) by letting $\varepsilon \rightarrow 0$, i.e., Find $(w, u) \in V \times Q$ such that

$$(3.8) \quad \begin{aligned} (w', v') + (u', v) &= (f, v) && \text{for all } v \in V = H_0^1(0, 1) \\ (w, q') &= 0 && \text{for all } q \in Q = H_0^1(0, 1). \end{aligned}$$

The problem is not well posed when $\int_0^1 f(x) dx \neq 0$. We can change the trial space Q to $L_0^2(0, 1) := \{u \in L^2(0, 1) \mid \int_0^1 u = 0\}$ in order to have existence and uniqueness of the solution. Nevertheless, in this case, the solution space cannot satisfy the boundary conditions of the original problem (1.2).

However, the *reduced discrete problem* obtained from (1.5) by letting $\varepsilon \rightarrow 0$, i.e., Find $(w_h, u_h) \in V_h \times \mathcal{M}_h$ such that

$$(3.9) \quad \begin{aligned} (w'_h, v'_h) + (u'_h, v_h) &= (f, v_h) && \text{for all } v_h \in V_h, \\ (w_h, q'_h) &= 0 && \text{for all } q_h \in \mathcal{M}_h, \end{aligned}$$

has unique solution. This is justified by the fact that a discrete inf – sup condition, using optimal trial norm on \mathcal{M}_h and the standard H^1 seminorm on V_h , holds.

Numerical tests in [5] showed that oscillation of the discrete solution u_h of (3.9) predict oscillatory behavior of the SPLS discrete solution u_h of (1.5). In fact, for $\varepsilon/h \leq 10^{-4}$, the two solutions look identical in the “eye ball measure”.

Next, we explain the solution behavior for the *reduced discrete problem* (3.9). We introduce $u^f \in V = H_0^1(0, 1)$ as the solution of

$$(3.10) \quad -(u^f)'' = f, \quad 0 < x < 1 \quad \text{or} \quad ((u^f)', v') = (f, v), \quad \text{for all } v \in V,$$

and the elliptic projection of u^f on $V_h = C^0 - P^2$, as the solution $u_h^f \in V_h$ of

$$(3.11) \quad ((u_h^f)', v_h') = (f, v_h), \quad \text{for all } v_h \in V_h.$$

In this section, we also need the solution $w(x) = \int_0^x f(s) ds$ of the (LR) transport problem (3.4), and the following two subspaces of $L^2(0, 1)$:

$$\begin{aligned} \overline{\mathcal{M}}_h &:= \{w_h - \bar{w}_h \mid w_h \in \mathcal{M}_h\}, \text{ and} \\ \tilde{\mathcal{M}}_h &:= \overline{\mathcal{M}}_h \bigoplus \text{span}\{1\} = \{v_h \in C^0 - P^1 \mid v_h(0) = v_h(1)\}. \end{aligned}$$

Next, we state the main result of this section.

Theorem 3.3. *Let u_h be the solution of the reduced discrete problem (3.9). Then, $u_h - \bar{u}_h$ is the $L^2(0, 1)$ orthogonal projection of $w(x) - \bar{w}$ onto $\tilde{\mathcal{M}}_h$.*

Proof. The system (3.9) is equivalent to

$$(3.12) \quad \begin{aligned} w_h + P_h T u_h &= u_h^f, \\ (w_h', q_h) &= 0 \quad \text{for all } q_h \in \mathcal{M}_h, \end{aligned}$$

where $\mathcal{M}_h = \text{span}\{\varphi_1, \dots, \varphi_{n-1}\}$, and P_h is the elliptic ptojection on V_h .

As presented in Section 3.2, $P_h T u_h = T u_h$ and $(T u_h)' = \bar{u}_h - u_h$. Differentiating the first equation of (3.12), we obtain

$$(3.13) \quad w_h' + \bar{u}_h - u_h = (u_h^f)'.$$

From the second equation of (3.12), using that $\int_0^1 w_h' = 0$, we have

$$(3.14) \quad (w_h', q_h - \bar{q}_h) = 0 \quad \text{for all } q_h \in \mathcal{M}_h.$$

By substituting w_h' from (3.13) in (3.14), we obtain

$$(3.15) \quad (u_h - \bar{u}_h, q_h - \bar{q}_h) = (-(u_h^f)', q_h - \bar{q}_h), \quad \text{for all } q_h \in \mathcal{M}_h.$$

Hence, $u_h - \bar{u}_h$ is the $L^2(0, 1)$ orthogonal projection of $-(u_h^f)'$ onto $\overline{\mathcal{M}}_h$.

Next, we prove that $u_h - \bar{u}_h$ is the $L^2(0, 1)$ orthogonal projection of $-(u^f)'$ onto $\overline{\mathcal{M}}_h$. We note that for any $q_h - \bar{q}_h \in \overline{\mathcal{M}}_h$, the function

$$v_h = \int_0^x (q_h(s) - \bar{q}_h) ds \in V_h = C^0 - P^2,$$

and

$$(3.16) \quad \begin{aligned} ((u_h^f)', q_h - \bar{q}_h) &= ((u_h^f)', (v_h)') = (f, v_h) \\ &= ((u^f)', (v_h)') = ((u^f)', q_h - \bar{q}_h). \end{aligned}$$

From (3.15) and (3.16), we have

$$(u_h - \bar{u}_h, q_h - \bar{q}_h) = (-(u^f)', q_h - \bar{q}_h), \quad \text{for all } q_h \in \mathcal{M}_h.$$

Thus, $u_h - \bar{u}_h$ is indeed the L^2 orthogonal projection of $-(u^f)'$ onto $\overline{\mathcal{M}}_h$. In addition, since $(u^f)'$ is L^2 orthogonal to constant functions, we also have that $u_h - \bar{u}_h$ is the L^2 orthogonal projection of $-(u^f)'$ onto $\tilde{\mathcal{M}}_h$.

Integrating $-(u^f)'' = f$ on $[0, x]$ gives us

$$-(u^f)'(x) = \int_0^x f(s) ds - (u^f)'(0) := w(x) - (u^f)'(0).$$

Integrating the above identity on $[0, 1]$ and using $(u^f)(0) = (u^f)(1) = 0$ give

$$(u^f)'(0) = \int_0^1 w(x) dx.$$

From the last two identities, we obtain

$$-(u^f)'(x) = w(x) - \bar{w},$$

and the theorem is proved. \square

Now, we justify the behavior of the solution u_h of the *reduced discrete problem* (3.9): When $\int_0^1 f(x) dx \neq 0$, the function $u_h - \bar{u}_h$ is the L^2 projection of the continuous function $w(x) - \bar{w}$ with different end values to a space $\tilde{\mathcal{M}}_h$ of continuous functions on $[0, 1]$ with the same values at the ends. For $f = 1$, we get $u^f = 0.5(x - x^2)$ and $w(x) - \bar{w} = x - 1/2$ which takes the values $\pm\frac{1}{2}$ at $x = 0$ and $x = 1$, respectively. Since functions in $\tilde{\mathcal{M}}_h$ have the same values at the ends, the L^2 orthogonal projection of $x - 1/2$ onto $\tilde{\mathcal{M}}_h$ oscillates at the ends, see Figure 3.1 (Left).

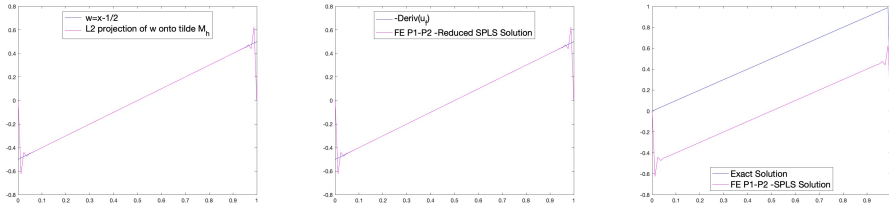


FIGURE 3.1. $n = 84$, Left: L^2 proj. of $w = x - 1/2$ on $\tilde{\mathcal{M}}_h$
 Middle: $P^1 - P^2$ SPLS for Reduced Problem
 Right: $P^1 - P^2$ SPLS for the Standard Problem, $\varepsilon = 10^{-6}$

When comparing the solution of the SL discretization to the discrete solution u_h of the standard SPLS formulation, we note that the discrete solution u_h is free of *global non-physical oscillations*, but exhibits *local oscillations* at the ends of the interval $[0, 1]$, see Figure 3.1 (Right). Numerical tests for the case $\int_0^1 f(x) dx \neq 0$ and $\varepsilon \ll h$ show that the SPLS discrete solution is very close to the solution of the *reduced discrete problem* (3.9). Both solutions, except for the end oscillations, are very close to the graph of the function

$$U(x) := w(x) - \frac{1}{2} w(1) = \int_0^x f - \frac{1}{2} \int_0^1 f = 1/2(w(x) + \theta(x)),$$

where w and θ are the solutions of the the RL and LR transport problems.

Remark 3.4. *The reduced problem (3.9) is independent of ε , and its solution can still exhibit oscillations. For $\varepsilon \ll h$, the reduced problem (3.9) predicts oscillatory behavior of the solution of the standard SPLS discretization (1.5). Oscillations at the boundary of the domain, appear because the discrete solution is approximated by an L^2 -projection of a continuous function with non-zero boundary conditions to a subspace of continuous functions that does not account for the boundary conditions of the function.*

Both SL and SPLS reduced discrete problems do not correspond to continuous reduced problems that have unique solutions.

For both SL and SPLS discretizations, the non-physical oscillations are related with the LR and RL transport problems. It has been proven in [12] that for $\varepsilon \ll h$, the exact solution u of (1.2) and the solution w of the LR transport problem are very close at the interior nodes x_1, x_2, \dots, x_{n-1} . We will address this idea again in Section 5.1. Thus, for any finite element discretization of (1.2), the closeness of the discrete solution u_h to w can lead to an oscillation free discretization. However, the “closeness” of u_h to the solution θ of the RL transport problem can lead to non-physical oscillations.

4. THE UPWINDING PETROV-GALERKIN METHOD WITH BUBBLE TYPE TEST SPACE

In this section, we review the one dimensional UPG method emphasizing on non-oscillatory behavior of the discrete solution. Our main idea of the bubble UPG method is to *choose the test space to create upwinding diffusion from the convection part*. To create a basis for the test space, for each nodal basis of the trial space, we add locally supported upwinding bubbles. The *upwinding process* leads to the elimination of the non-physical oscillation in the discrete solutions, and to better approximation.

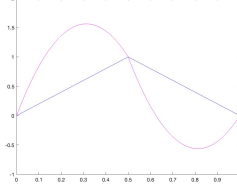
To be more precise, we define the test space V_h by introducing a bubble function for each interval $[x_{i-1}, x_i]$, $i = 1, 2, \dots, n$. First, consider a *bubble generating function* $B : [0, h] \rightarrow \mathbb{R}$ with the following properties:

$$B(0) = B(h) = 0, \quad \frac{1}{h} \int_0^h B = b, \quad \text{and} \quad \int_0^h (B'(x))^2 dx = \frac{b_e}{h} \quad \text{with } b, b_e > 0.$$

Next, for $i = 1, \dots, n$, define $B_i : [0, 1] \rightarrow \mathbb{R}$ by $B_i(x) = B(x - x_{i-1})$ on $[x_{i-1}, x_i]$, and extend it by zero to the entire interval $[0, 1]$. The discrete test space for the bubble UPG discretization is

$$V_h := \text{span}\{g_i : i = 1, 2, \dots, n-1\}, \quad \text{where } g_i = \varphi_i + (B_i - B_{i+1}).$$

The idea of bubble enriched test spaces was introduced for quadratic bubbles in [16]. A generalization of the method, using an arbitrary generating bubble function, is presented and analyzed in [4, 5]. A particular choice for the generating bubble B is $B = 4\varphi_0\varphi_1 = 4\frac{x}{h}(1 - \frac{x}{h})$. In this case, the graphs of a basis trial function φ_i and a basis test function $g_i = \varphi_i + (B_i - B_{i+1})$ are presented below.



The bubble UPG idea for solving (1.2) resides in the choice of the signs of the added bubbles in order to match the convection coefficient $1 > 0$.

The upwinding Petrov Galerkin discretization with general bubble functions for (1.2) is: Find $u_h \in \mathcal{M}_h$ such that

$$(4.1) \quad b(v_h, u_h) = \varepsilon a_0(u_h, v_h) + (u'_h, v_h) = (f, v_h) \quad \text{for all } v_h \in V_h.$$

As presented in [12, 15], by writing a generic test function $v_h \in V_h$ as $v_h = w_h + B_h \in V_h$, with $w_h \in \mathcal{M}_h$ the linear part of v_h , and B_h the bubble part of v_h , the problem (4.1) with $V_h := \text{span}\{g_i\} = \text{span}\{\varphi_i + (B_i - B_{i+1})\}$ has the reformulation: Find $u_h \in \mathcal{M}_h = C^0 - P^1$ such that

$$(4.2) \quad \begin{aligned} & (\varepsilon + b h) (u'_h, w'_h) + (u'_h, w_h) = F_{upg}(w_h), \text{ where} \\ & F_{upg}(w_h) := (f, w_h) + h (f, w'_h \sum_{i=1}^n B_i), w_h \in \mathcal{M}_h. \end{aligned}$$

Note that the bubble part B_h in the convection term of the original variational formulation, i.e., (u'_h, B_h) , produces the extra diffusion term $b h (u'_h, w'_h)$. In other words, the bubble part of the test space creates *upwinding diffusion* from the convection term. This is an important feature of the bubble UPG method that can be extended to the multidimensional case.

The reformulation (4.2) involves only linear functions in the bilinear form. From (4.2), it is easy to check that the matrix associated with the reformulation is tridiagonal. More precisely,

$$(4.3) \quad M_{fe} = \text{tridiag} \left(-\left(\frac{\varepsilon}{h} + b\right) - \frac{1}{2}, 2\left(\frac{\varepsilon}{h} + b\right), -\left(\frac{\varepsilon}{h} + b\right) + \frac{1}{2} \right),$$

and depends only on ε, h and the average b of the generating bubble B .

Based on the reformulation (4.2), we proved the following error estimate in the discrete optimal trial norm, in [12, 15].

Theorem 4.1. *If u is the solution of (3.1), u_h is the solution of the upwinding PG formulation (4.1), and the bubble B is chosen such that $b \geq 1/\pi$, then*

$$(4.4) \quad \|u - u_h\|_{*,h} \leq \sqrt{1 + b_e} \inf_{p_h \in \mathcal{M}_h} \|u - p_h\|_{*,h} \leq \sqrt{1 + b_e} \|u - I_h(u)\|_{*,h},$$

where $I_h(u)$ is the linear interpolant of u on the uniform mesh of size h ,

$$\|u_h\|_{*,h}^2 = \frac{(\varepsilon + h b)^2}{1 + b_e} |u_h|^2 + \frac{1}{1 + b_e} |u_h|_{*,h}^2,$$

and $|\cdot|_{*,h}$ is the seminorm defined in (2.9).

Note that the “teeth saw” function ω_h satisfies $|\omega_h|_{*,h}^2 = 0$, $|\omega_h|^2 = 1/h^2$. Hence,

$$\|\omega_h\|_{*,h}^2 = \frac{1}{1 + b_e} \frac{(\varepsilon + h b)^2}{h^2} \geq \frac{b^2}{1 + b_e} \text{ and}$$

the discrete solution could not contain spurious modes of “teeth saw” type.

The error estimate (4.4) is quasi-optimal in the discrete optimal norm, but it essentially depends on the approximation properties of the linear interpolant on uniform meshes. Since, in general, the solution u exhibits a boundary layer close to $x = 1$, the interpolant of u fails to approximate well the exact solution on regions close to $x = 1$. Thus, the global estimate (4.4) might not be able to control the discrete infinity error, and therefore, the oscillatory behavior of the discrete solution.

However, for special choices of the generating bubble function B , we can control the discrete infinity error of the bubble UPG method. For example, we can choose a bubble B with the average $b = \frac{1}{2} - \frac{\varepsilon}{h}$, such that the upper diagonal entries in the matrix M_{fe} are zero. The matrix $M = M_{fe}$ becomes:

$$(4.5) \quad M = \text{tridiag}(-1, 1, 0),$$

and the linear system corresponding to (4.2) is

$$M U = F_{pg}, \text{ where } F_{pg} = [(f, g_1), (f, g_2), \dots, (f, g_{n-1})]^T.$$

A forward solve leads to the following formula for the component u_j of U :

$$(4.6) \quad u_j = (f, \varphi_1 + \varphi_2 + \dots + \varphi_j) + (f, B_1 - B_{j+1}), \quad j = 1, 2, \dots, n-1.$$

Introducing the nodal function φ_0 corresponding to $x_0 = 0$, i.e., φ_0 is the continuous piecewise linear function on $[0, 1]$ such that $\varphi_0(x_j) = \delta_{0,j}$, $j = 0, 1, \dots, n$, and using that $\varphi_0 + \varphi_1 + \dots + \varphi_j = 1$ on $[0, x_j]$, the formula (4.6) leads to

$$(4.7) \quad u_j = \int_0^{x_j} f(x) \, dx + \int_0^{x_1} f(B_1 - \varphi_0) \, dx + \int_{x_j}^{x_{j+1}} f(\varphi_j - B_{j+1}) \, dx,$$

Similar with a special case of quadratic UPG presented in [12], we have:

Theorem 4.2. *Assume that $f \in C([0, 1])$ and $u_h = \sum_{j=1}^{n-1} u_j \varphi_j$ is the solution of the UPG formulation (4.1), with the bubble function B chosen such that $b = \frac{1}{2} - \frac{\varepsilon}{h} > 0$. Then,*

$$\left| u_j - \int_0^{x_j} f(x) \, dx \right| \leq 2 \|f\|_\infty \left(1 - \frac{\varepsilon}{h} \right) h \leq 2 \|f\|_\infty h.$$

Proof. We note that

$$\int_0^{x_1} B_1 \, dx = \int_{x_j}^{x_{j+1}} B_{j+1} \, dx = \left(\frac{1}{2} - \frac{\varepsilon}{h} \right) h, \text{ and } \int_0^{x_1} \varphi_1 \, dx = \int_{x_j}^{x_{j+1}} \varphi_j = \frac{h}{2}.$$

Thus, using the formulas (4.7) and the triangle inequality, we have

$$\begin{aligned} & \left| u_j - \int_0^{x_j} f(x) \, dx \right| = \\ & \left| \int_0^{x_1} f(B_1 - \varphi_0) \, dx + \int_{x_j}^{x_{j+1}} f(\varphi_j - B_{j+1}) \, dx \right| \leq \|f\|_\infty \left(2 - \frac{2\varepsilon}{h} \right) h. \end{aligned}$$

□

Consequently, for $j = 1, \dots, n-1$, the components u_j of the UPG solution approximate $w(x_j) = \int_0^{x_j} f(x) \, dx$ with order $\mathcal{O}(h)$. If f is independent of ε and $h > \varepsilon$, then the UPG solution is $\mathcal{O}(h)$ close to the solution of the transport problem (3.4) at the interior nodes, hence free of non-physical oscillations. As mentioned before, for $\varepsilon \ll h$ and for $j = 1, 2, \dots, n-1$, the values $w(x_j)$ are very close to $u(x_j)$, where u is the exact solution of (1.2). Thus, at least for $\varepsilon \ll h$, the discretization approximates well the exact solution at the interior nodes. In Section 5, we show that, for different generating bubbles B , we can provide precise discrete infinity norm error estimates for the UPG method.

5. THE IMPORTANCE OF THE DISCRETE INFINITY ERROR CONTROL

Many finite element discretizations of convection dominated problems, including the Streamline Upwind Petrov–Galerkin (SUPG), SPLS and Streamline Diffusion (SD), exhibit non-physical oscillations. For such methods, the convergence analysis was done in various weighted energy norms that include L^2 and H^1 terms and the error estimates were done on the entire domain of the problem, including on regions corresponding to boundary layers. When considering such energy norms, the best approximation of the finite element solution is usually estimated by using the approximation properties of the interpolant in L^2 and H^1 norms. The interpolant approximation error could be large, especially on subdomains containing the boundary layer.

As an example of possible large magnitude for $|u - I_h(u)|$, we considered $f = 1$ in (1.2) with the exact solution $u(x) = x - (e^{\frac{x}{\varepsilon}} - 1)/(e^{\frac{1}{\varepsilon}} - 1)$. As presented in [2], the linear interpolant of u on the uniform mesh of size h satisfies

$$\begin{aligned} |u - I_h(u)|_{[0,1]}^2 &= \frac{1 + e^{-1/\varepsilon}}{1 - e^{-1/\varepsilon}} \left(\frac{1}{2\varepsilon} - \frac{1}{h} \frac{1 - e^{-h/\varepsilon}}{1 + e^{-h/\varepsilon}} \right) \approx \frac{1}{2\varepsilon} - \frac{1}{h}, \text{ for } \varepsilon \ll h, \\ |u - I_h(u)|_{[0,1-h]}^2 &= \frac{e^{-2h/\varepsilon} - e^{-2/\varepsilon}}{1 - e^{-2/\varepsilon}} |u - I_h(u)|_{[0,1]}^2 \approx e^{-2h/\varepsilon} |u - I_h(u)|_{[0,1]}^2. \end{aligned}$$

Thus, for $\varepsilon \ll h$, we have

$$\begin{aligned} |u - I_h(u)|_{[0,1-h]} &\approx e^{-h/\varepsilon} |u - I_h(u)|_{[0,1]} \approx 0, \text{ and} \\ |u - I_h(u)|_{[1-h,1]}^2 &\approx |u - I_h(u)|_{[0,1]}^2 \approx \frac{1}{2\varepsilon} - \frac{1}{h}. \end{aligned}$$

These estimates show that, for $\varepsilon \ll h$, the interpolant's energy error $|u - I_h(u)|$ is insignificantly small on the interval $[0, 1 - h]$, is very large on $[0, 1]$, and is essentially attained on the last mesh-interval $[1 - h, 1]$. Thus, energy type error estimates are not suitable to provide higher order of approximation of the solution. Therefore, they are not able to predict non-physical oscillations of the discrete solution.

5.1. The importance of convergence in discrete infinity error norm.

The idea of controlling the discrete infinity error in the convergence analysis for convection diffusion problems can be found in the context of monotone schemes discretization, as presented for example in [25].

In order for a continuous piecewise linear approximation u_h of the solution u of a convection dominated problem to be oscillation free, it would be enough to have that $\|u_h - I_h(u)\|_{h,\infty}$ converges fast to zero, as $h \rightarrow 0$. Here,

$$\|u_h - I_h(u)\|_{h,\infty} := \max\{|u_h(x_j) - u(x_j)| : x_j \in \Omega, x_j - \text{mesh node}\}.$$

This is also known as *the closeness property* of the discrete solution.

For example, let us assume that for a particular discrete solution $u_h \in \mathcal{M}_h = C^0 - P^1$, we have

$$\|u_h - I_h(u)\|_{h,\infty} \leq \mathcal{O}(h^2).$$

For functions in \mathcal{M}_h , by using standard inverse inequality estimates that hold with constants independent of h and ε , we also have

$$(5.1) \quad h |u_h - I_h(u)| \preceq \|u_h - I_h(u)\| \preceq \|u_h - I_h(u)\|_{h,\infty}.$$

Consequently, the splitting $u_h - u = (u_h - I_h(u)) + (I_h(u) - u)$ leads to optimal error estimates for $|u_h - u|$ and $\|u - u_h\|$ *away from the boundary layers* (ABL). Here, we can define ABL as any subdomain region on which the H^1 or L^2 interpolation errors maintain optimal order for the exact solution, and the error estimates are independent of ε .

In conclusion, controlling the discrete infinity error eliminates oscillations and could lead to optimal L^2 and H^1 error estimates, ABL. The norm estimate (5.1) is independent of the problem dimension, hence the ideas of this section can be extended to *multidimensional* convection-diffusion problems.

5.2. The exponential bubble UPG provides the exact solution at the nodes.

In [12], we analyzed an UPG discretization for (1.2), using the special exponential generating bubble function $B : [0, h] \rightarrow \mathbb{R}$ defined by

$$(5.2) \quad B(x) = B^e(x) := \frac{1 - e^{-\frac{x}{\varepsilon}}}{1 - e^{-\frac{h}{\varepsilon}}} - \frac{x}{h}.$$

Introducing the notation $t_0 := \tanh(\frac{h}{2\varepsilon})$, we get $b = \frac{1}{h} \int_0^h B(x) dx = \frac{1}{2t_0} - \frac{\varepsilon}{h}$ and

$$(5.3) \quad M_{fe} = M_{fe}^e = \frac{1}{t_0} \text{tridiag} \left(-\frac{1+t_0}{2}, 1, -\frac{1-t_0}{2} \right).$$

It has been shown that the exponential bubble UPG recovers the exact solution u at the mesh nodes, see [12] and [23].

Next, we emphasize that, for $\varepsilon \ll h$, at the interior nodes, the exponential bubble UPG solution is also very close to the solution of the LR transport problem (3.4). For $\frac{\varepsilon}{h} \rightarrow 0$, we have *with fast convergence* that

$$t_0 \rightarrow 1, \text{ and } g_j = \varphi_j + B_j^e - B_{j+1}^e \rightarrow \chi_{[x_{j-1}, x_j]}.$$

Consequently, we have *with fast convergence* that

$$M_{fe} \rightarrow \text{tridiag}(-1, 1, 0), \text{ and } (f, g_j) \rightarrow \int_{x_{j-1}}^{x_j} f(x) dx.$$

Thus, for $\varepsilon \ll h$, the matrix M_{fe}^e is very close to $\text{tridiag}(-1, 1, 0)$, and the *reduced linear system* becomes

$$[\text{tridiag}(-1, 1, 0)] W = \left[\int_{x_0}^{x_1} f(x) dx, \dots, \int_{x_{n-2}}^{x_{n-1}} f(x) dx \right]^T.$$

By forward solving the linear system, we obtain

$$w_j = \int_0^{x_j} f(x) dx, \quad j = 1, 2, \dots, n-1.$$

This implies that the component u_j of the UPG discrete solution is very close or identical to the value $w(x_j) = \int_0^{x_j} f(t) dt$. In conclusion, we have:

Remark 5.1. *The reduced linear system obtained from taking the limit as $\varepsilon/h \rightarrow 0$ in the linear system for the exponential bubble UPG method, represents a discretization of the LR transport problem (3.4), which has unique solution. For $\varepsilon \ll h$, at the interior nodes, the exact solution is very close to the solution w of (3.4).*

Another benefit of the exponential bubble UPG method, is that, using the Green's function for the problem (1.2), i.e.,

$$G(x, s) = \frac{1}{e^{\frac{1}{\varepsilon}} - 1} \begin{cases} (e^{\frac{1}{\varepsilon}} - e^{\frac{x}{\varepsilon}})(1 - e^{-\frac{s}{\varepsilon}}), & 0 \leq s < x, \\ (e^{\frac{x}{\varepsilon}} - 1)(e^{\frac{1-s}{\varepsilon}} - 1), & x \leq s \leq 1, \end{cases}$$

we have an *exact formula for the inverse of the UPG discretization matrix*:

$$(5.4) \quad M_{fe}^{-1} = [G(x_j, x_i)]_{i,j=1,2,\dots,n-1}.$$

Consequently, for any inside node x_j , the UPG solution u_h is given by

$$(5.5) \quad u_h(x_j) = u(x_j) = \sum_{i=1}^{n-1} G(x_j, x_i) (f, \varphi_i + B_i^e - B_{i+1}^e).$$

The formula allows for discrete infinity error analysis for other bubble UPG methods. Details of the proofs are given in [2].

5.3. Properly scaled quadratic bubble UPG provides optimal approximation. Working with exponential bubble functions could lead to difficulties in computing the right hand side dual vectors. A *properly scaled quadratic bubble UPG* can be used to obtain $\mathcal{O}(h^2)$ approximation of the exact solution in the *discrete infinity norm*. We choose the generating bubble function

$$B(x) = B^q(x) := \frac{4\beta}{h^2}x(h-x), \text{ with } \beta = \frac{3}{2} \left(\frac{1}{2t_0} - \frac{\varepsilon}{h} \right),$$

such that the quadratic bubble B^q and the exponential bubble B^e have the same average b . The stiffness matrix formula (4.3) gives that the quadratic and exponential UPG discretizations lead to the same linear system matrix. From (5.4), we get that for any inside node x_j , the quadratic bubble solution u_h is given by

$$(5.6) \quad u_h(x_j) = \sum_{i=1}^{n-1} G(x_j, x_i) (f, \varphi_i + B_i^q - B_{i+1}^q).$$

By using the solution formulas (5.5) and (5.6) and standard linear algebra arguments, we obtain the following result.

Theorem 5.2. *If $u_h = \sum_{j=1}^{n-1} u_j \varphi_j$ is the quadratic bubble UPG solution with $\beta = \frac{3}{2} \left(\frac{1}{2t_0} - \frac{\varepsilon}{h} \right)$, and $e^{-\frac{\varepsilon}{h}} \leq h$, then*

$$\|u_h - I_h(u)\|_{h,\infty} := \max |u(x_j) - u_j| \leq 2\varepsilon \|f\|_\infty + \frac{h^2}{4} \|f'\|_\infty.$$

The proof can be found in [2]. The estimate is a sharp result, especially if $\|f\|_\infty$ and $\|f'\|_\infty$ can be bounded independently of ε .

For $\varepsilon \leq h^2$, the theorem gives $\|u_h - I_h(u)\|_{h,\infty} \leq Ch^2$, with precise control of the constant C . In addition, according to Section 5.1, the estimate leads to

$$|u - u_h| \leq \mathcal{O}(h), \text{ and } \|u - u_h\|_{L^2} \leq \mathcal{O}(h^2) \text{ away from the boundary layer.}$$

Remark 5.3. *We note that it is essential to use the scaling $\beta = \frac{3}{2} \left(\frac{1}{2t_0} - \frac{\varepsilon}{h} \right)$ in order to obtain optimal approximation in the discrete infinity norm. Otherwise, the H^1 and L^2 errors increase and the orders of convergence decrease, especially for the L^2 error.*

The strategy of properly scaling the generating bubble function could be used to obtain *discrete infinity error estimates for the two dimensional case* as well.

6. TWO DIMENSIONAL EXTENSIONS OF BUBBLE UPG DISCRETIZATIONS

The bubble UPG idea can be extended to multidimensional case of problem (1.1). In [2], we described the extension ideas for $\Omega = (0, 1) \times (0, 1)$ and $\mathbf{b} = [1, 0]$. In this case, the problem (1.1) becomes: Find $u = u(x, y)$ such that

$$(6.1) \quad \begin{cases} -\varepsilon \Delta u + u_x = f & \text{in } \Omega, \\ u = 0 & \text{on } \partial\Omega. \end{cases}$$

It is known that the general solution of (6.1) could exhibit both elliptic and parabolic boundary layers, see e.g., [23]. The following general bubble UPG in the x -direction discretization was considered in [2]. With the notation of Section 4, using a generating bubble $B = B(x)$, we define the trial and test spaces by:

$$\mathcal{M}_h = \text{span}\{\varphi_i(x)\varphi_j(y), \text{ for all } (x_i, x_j) \in \Omega\}, \text{ and}$$

$$V_h = \text{span}\{(\varphi_i(x) + B_i(x) - B_{i+1}(x))\varphi_j(y), \text{ for all } (x_i, x_j) \in \Omega\}.$$

A general UPG discretization with bubble functions in the x -direction for solving (6.1) is: Find $u_h \in \mathcal{M}_h$ such that

$$(6.2) \quad b(v_h, u_h) := \varepsilon (\nabla u_h, \nabla v_h) + \left(\frac{\partial u_h}{\partial x}, v_h \right) = (f, v_h) \quad \text{for all } v_h \in V_h.$$

For defining the UPG with *quadratic bubble upwinding*, we choose

$$B(x) = B^q(x) = \frac{4\beta}{h^2}x(h-x), \text{ with the matching } \beta = \frac{3}{2} \left(\frac{1}{2t_0} - \frac{\varepsilon}{h} \right).$$

In this section, we will focus on understanding the oscillation spikes for the quadratic UPG discretization of (6.1) along the parabolic boundary layers.

Numerical tests for examples with elliptic Boundary Layers (BL), show that, for $\varepsilon \leq h^2$ as in the one dimensional case, the *UPG solution* u_h , satisfies

$$(6.3) \quad \|u_h - I_h(u)\|_{h,\infty} = \mathcal{O}(h^2), \text{ and}$$

$$(6.4) \quad |u - u_h| = \mathcal{O}(h), \text{ and } \|u - u_h\|_{L^2} = \mathcal{O}(h^2),$$

away from the *elliptic boundary layer*, see [2]. In addition, if the H^1 and L^2 errors are computed on the whole domain, we notice that the orders of convergence decrease. However, in this case of for $\varepsilon \leq h^2$, we get

$$(6.5) \quad |u - u_h| \approx |I_h(u) - u_h|, \text{ and } \|u - u_h\|_{L^2} \approx \|I_h(u) - u_h\|_{L^2}.$$

Numerical tests for examples with elliptic BL near $x = 1$ and parabolic BLs near $y = 0$ and $y = 1$ showed that the estimate (6.3) also holds for $\varepsilon \leq h^2$, but only *away from the parabolic BL*, and that (6.4) still holds away from both elliptic and parabolic boundary layers.

The numerical solution for $f = 1$ (for which the solution exhibits both types of BL) has *no spikes for $\varepsilon > h^2$* , but exhibits *non-physical spikes* for $\varepsilon \ll h^2$ near $y = 0$ and $y = 1$, see Figure 6.1 (Left plot). Other discretization methods, including SUPG, show similar behavior for $\varepsilon \ll h^2$.

In [20] and many of the references therein, various stabilization methods were introduced in order to try eliminating such oscillations.

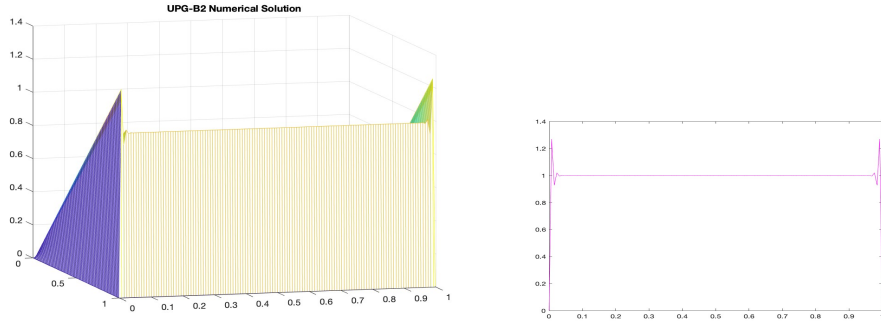


FIGURE 6.1. The quadratic UPG solution, $\varepsilon = 10^{-7}$, $h = 1/2^7$, and the L^2 orthogonal projection of $1_{[0,1]}$ on \mathcal{M}_h .

6.1. Understanding the oscillation spikes near the parabolic BLs.

We provide an explanation of spikes along parabolic BLs for the 2D scaled *quadratic bubble UPG method*, based on investigating the tensor structure of the resulting linear system. The linear system corresponding to (6.2) is

$$(6.6) \quad A^q U^q = F^q, \text{ where } A^q = M \otimes M_{fe}^e + \frac{\varepsilon}{h} S \otimes M^q.$$

Here, $M = [(\varphi_i, \varphi_j)]_{i,j=1,\dots,n-1} = \frac{h}{6} \text{tridiag}(1, 4, 1)$ is the one dimensional mass matrix,

$$S = \text{tridiag}(-1, 2, -1), \text{ and } M^q = M + \beta(h/3) \text{tridiag}(-1, 0, 1),$$

$$U^q = [u_{11}, \dots, u_{n-1,1}, u_{12}, u_{22}, \dots, u_{n-1,2}, \dots, u_{n-1,n-1}]^T,$$

$$F^q = [(f, g_1^q \varphi_1), \dots, (f, g_{n-1}^q \varphi_1), (f, g_1^q \varphi_2), \dots, (f, g_{n-1}^q \varphi_{n-1})]^T,$$

u_{ij} corresponds to the node (x_i, x_j) , and $g_i^q = \varphi_i + B_i^q - B_{i+1}^q$.

Next, we note that

$$\lim_{\varepsilon/h \rightarrow 0} M_{fe}^e = C^0 := \text{tridiag}(-1, 1, 0), \text{ and } \lim_{\varepsilon/h \rightarrow 0} B^q \rightarrow B^{q_0} := 3 \frac{x}{h} \left(1 - \frac{x}{h}\right).$$

By taking the limit as $\varepsilon/h \rightarrow 0$ in the system (6.6), we obtain the *reduced linear system*

$$(6.7) \quad [M \otimes C^0] W = F^{q_0}, \text{ where}$$

$$F^{q_0} = [(f, g_1^{q_0} \varphi_1), \dots, (f, g_{n-1}^{q_0} \varphi_1), (f, g_1^{q_0} \varphi_2), \dots, (f, g_{n-1}^{q_0} \varphi_{n-1})]^T,$$

and $g_i^{q_0} = \varphi_i + B_i^{q_0} - B_{i+1}^{q_0}$.

For $\varepsilon \ll h$, the solution U^q of (6.6) is very close to the solution W of the *reduced linear system* (6.7). The solution of the linear system (6.7) is

$$(6.8) \quad W = [M^{-1} \otimes (C^0)^{-1}] F^{q_0}.$$

By using that

$$\int_0^{x_1} B_1^{q_0}(x) dx = \int_{x_j}^{x_{j+1}} B_{j+1}^{q_0}(x) dx = \frac{h}{2} = \int_0^h \varphi_0(x) dx = \int_{x_j}^{x_{j+1}} \varphi_{j+1} dx,$$

and (6.8), for $f = 1$ we obtain that, for each $i = 1, \dots, n-1$ the x_i -section of W satisfies

$$[w_{i1}, \dots, w_{i,n-1}]^T = M^{-1} \left[\left(\int_0^{x_i} 1 ds, \varphi_1(y) \right), \dots, \left(\int_0^{x_i} 1 ds, \varphi_{n-1}(y) \right) \right]^T.$$

Since M is the one dimensional mass matrix, the above inversion represents the projection of the constant function $x_i 1_{[0,1]}$ to $\text{span}\{\varphi_1(y), \dots, \varphi_{n-1}(y)\}$. Figure 6.1, shows the quadratic UPG solution for a case $\varepsilon \ll h$ versus the one dimensional L^2 projection of the constant function $1_{[0,1]}$ onto \mathcal{M}_h . It is interesting to see that the graph of the L^2 projection is scaled down to generate the quadratic UPG solution, when x goes from $1-h$ to 0. This shows that the UPG oscillations in the case $\varepsilon \ll h$ are due to the one dimensional projection of a function that is not zero at the ends onto the space \mathcal{M}_h of continuous piecewise linear functions *with zero boundary conditions*.

We also note that the the x_i -section of W , the solution of the *reduced linear system* (6.7), is approximated by the projection of $\int_0^{x_i} f(s, y) ds$ on $\mathcal{M} = \mathcal{M}(y)$. Thus, W corresponds to a discretization of the *continuous transport problem*: Find $w \in H^1(\Omega)$ such that

$$(6.9) \quad \begin{cases} w_x = f & \text{in } \Omega, \\ w = 0 & \text{for } x = 0, y = 0, \text{ and } y = 1. \end{cases}$$

If $f \in C^1([0,1] \times [0,1])$ and $f(x, 0) = f(x, 1) = 0$ for all $x \in [0, 1]$, then the exact solution of (6.9) is $w(x, y) = \int_0^x f(s, y) ds$ for all $(x, y) \in \Omega$. On the other hand, if $f \in C^1([0,1] \times [0,1])$, but $f(x, 0) \neq 0$ or $f(x, 1) \neq 0$ for some $x \in [0, 1]$, for example $f = 1$, then (6.9) might not have a solution in $H^1(\Omega)$.

7. CONCLUSIONS ON OSCILLATORY BEHAVIOR OF CONVECTION-DIFFUSION DISCRETIZATION

This paper addresses the oscillatory behavior of certain finite element discretizations for a model convection-diffusion problem. The work identifies the causes of non-physical oscillations of finite element approximation of convection dominated problems, and suggests ways to avoid such behavior. For the bubble UPG method, we emphasize on a new approach for conducting error analysis that starts with establishing the *closeness* of the discrete solution first, followed by using inverse inequalities to establish approximation estimates in standard L^2 and H^1 norms, away from boundary layers. The ideas presented here can be used in building new discretizations that are free of non-physical oscillations for the multi-dimensional convection dominated problems.

Here are the conclusions that follow from the work in this paper, intertwined with related work presented in [2, 5, 12, 15].

- 1) The behavior of *the reduced discrete problem* obtained by letting $\varepsilon \rightarrow 0$ in the discrete variational formulation, *predicts the numerical pollution* for the case $\varepsilon \ll h$.
- 2) To avoid oscillations for discretizations of a convection dominated problem, *the reduced discrete problem* should have unique solution and should correspond to a continuous problem that has unique solution, for example, a related transport equation.
- 3) In the one dimensional case, to eliminate the non-physical solutions for the *standard linear* discretization or the *saddle point least square* discretization, one can split the data $f = (f - \bar{f}) + \bar{f}$, and solve the two corresponding problems for $f - \bar{f}$ and \bar{f} . The solution for a constant data \bar{f} can be found explicitly. The data $f - \bar{f}$ has average zero, and both continuous and discrete corresponding reduced problems have unique solutions.
- 4) Local oscillations at the boundary of the domain, can appear because the discrete solution is approximated by an L^2 -projection of continuous functions with non-zero boundary conditions, to conforming subspaces that do not account for the boundary conditions.
- 5) For the one dimensional quadratic bubble UPG method, the special scaling of the bubble leads to an optimal convergence estimate in the discrete infinity norm, and leads to optimal error estimates in the standard H^1 and L^2 norms, away from the boundary layers.
- 6) For the two dimensional bubble UPG and a given ε , by choosing h such that $h^2 \approx \varepsilon$, the discrete solution is free of non-physical oscillations and approximates well the exact solution in both H^1 and L^2 norms, *away from all boundary layers*.
- 7) The discretization of multi-dimensional convection dominated problems, could *benefit from the efficient discretization of the corresponding one dimensional problem along each stream line*. We can construct discrete test spaces by a “tensor type” construction using UPG discretization along the stream line direction and *standard discretizations on the orthogonal direction(s)*.
- 8) To eliminate non-physical oscillations, it is desirable to have a discretization that satisfies a *closeness property* such as

$$\|u_h - I_h(u)\|_{h,\infty} \approx \mathcal{O}(h^\alpha), \text{ with } \alpha > 1.$$

Once this is achieved, the estimate can be combined with standard inverse inequalities to prove error estimates for $|u - u_h|$ and $\|u - u_h\|_{L^2}$, *away from the boundary layers*.

REFERENCES

- [1] A. Aziz and I. Babuška. Survey lectures on mathematical foundations of the finite element method. *The Mathematical Foundations of the Finite Element Method with Applications to Partial Differential Equations*, A. Aziz, editor, 1972.
- [2] C. Bacuta. On convergence of upwinding Petrov-Galerkin methods for convection-diffusion. *submitted to Applicable Analysis*. arXiv:2509.04703, September 4, 2025.
- [3] C. Bacuta. Schur complements on Hilbert spaces and saddle point systems. *J. Comput. Appl. Math.*, 225(2):581–593, 2009.
- [4] C. Bacuta, D. Hayes, and O’Grady. Notes on finite element discretization for a model convection-diffusion problem. *preprint*, arXiv:2302.07809:1–24, 2023.
- [5] C. Bacuta, D. Hayes, and O’Grady. Saddle point least squares discretization for convection-diffusion. *Appl. Anal.*, 103(12):2241–2268, 2024.
- [6] C. Bacuta and J. Jacavage. A non-conforming saddle point least squares approach for an elliptic interface problem. *Comput. Methods Appl. Math.*, 19(3):399–414, 2019.
- [7] C. Bacuta and J. Jacavage. Saddle point least squares preconditioning of mixed methods. *Computers & Mathematics with Applications*, 77(5):1396–1407, 2019.
- [8] C. Bacuta and J. Jacavage. Least squares preconditioning for mixed methods with nonconforming trial spaces. *Applicable Analysis*, 99(16):2755–2775, 2020.
- [9] C. Bacuta and P. Monk. Multilevel discretization of symmetric saddle point systems without the discrete LBB condition. *Appl. Numer. Math.*, 62(6):667–681, 2012.
- [10] C. Bacuta and K. Qirko. A saddle point least squares approach to mixed methods. *Comput. Math. Appl.*, 70(12):2920–2932, 2015.
- [11] C. Bacuta and K. Qirko. A saddle point least squares approach for primal mixed formulations of second order PDEs. *Comput. Math. Appl.*, 73(2):173–186, 2017.
- [12] Cr. Bacuta and C. Bacuta. Connections between finite difference and finite element approximations for a convection-diffusion problem. *Revue Roumaine de Mathematique Pures et Appliques*, 69(3–4):353–374, 2024.
- [13] D. Boffi, F. Brezzi, L. Demkowicz, R. G. Durán, R. Falk, and M. Fortin. *Mixed finite elements, compatibility conditions, and applications*, volume 1939 of *Lecture Notes in Mathematics*. Springer-Verlag, Berlin; Fondazione C.I.M.E., Florence, 2008. Lectures given at the C.I.M.E. Summer School held in Cetraro, June 26–July 1, 2006, Edited by Boffi and Lucia Gastaldi.
- [14] D. Boffi, F. Brezzi, and M. Fortin. *Mixed finite element methods and applications*, volume 44 of *Springer Series in Computational Mathematics*. Springer, Heidelberg, 2013.
- [15] Cr. Bacuta C. Bacuta and D. Hayes. Comparison of variational discretizations for a convection-diffusion problem. *Revue Roumaine de Mathematique Pures et Appliques*, 69(3–4):327–351, 2024.
- [16] I. Christie, D. F. Griffiths, A. R. Mitchell, and O. C. Zienkiewicz. Finite element methods for second order differential equations with significant first derivatives. *Internat. J. Numer. Methods Engrg.*, 10(6):1389–1396, 1976.
- [17] A. Cohen, W. Dahmen, and G. Welper. Adaptivity and variational stabilization for convection-diffusion equations. *ESAIM Math. Model. Numer. Anal.*, 46(5):1247–1273, 2012.
- [18] L. Demkowicz, T. Führer, N. Heuer, and X. Tian. The double adaptivity paradigm (how to circumvent the discrete inf-sup conditions of Babuška and Brezzi). Technical report, 2021.
- [19] K. Eriksson, D. Estep, P. Hansbo, and C. Johnson. *Computational differential equations*. Cambridge University Press, Cambridge, 1996.
- [20] Petr Knobloch. On the choice of the supg parameter, at outflow boundary layers. *Adv. Comput. Math.*, 31(4):369–389, 2009.

- [21] R. Lin and M. Stynes. A balanced finite element method for singularly perturbed reaction-diffusion problems. *SIAM Journal on Numerical Analysis*, 50(5):2729–2743, 2012.
- [22] T. Linß. *Layer-adapted meshes for reaction-convection-diffusion problems*, volume 1985 of *Lecture Notes in Mathematics*. Springer-Verlag, Berlin, 2010.
- [23] H.-G. Roos, M. Stynes, and L. Tobiska. *Numerical methods for singularly perturbed differential equations*, volume 24 of *Springer Series in Computational Mathematics*. Springer-Verlag, Berlin, 1996. Convection-diffusion and flow problems.
- [24] H.G. Roos and M. Schopf. Convergence and stability in balanced norms of finite element methods on Shishkin meshes for reaction-diffusion problems: Convergence and stability in balanced norms. *ZAMM Journal of applied mathematics and mechanics: Zeitschrift für angewandte Mathematik und Mechanik*, 95(6):551–565, 2014.
- [25] J. Xu and L. Zikatanov. A monotone finite element scheme for convection diffusion equations. *Math. Comp.*, 68(228):1429–1446, 2000.
- [26] J. Xu and L. Zikatanov. Some observations on Babuška and Brezzi theories. *Numer. Math.*, 94(1):195–202, 2003.
- [27] O. C. Zienkiewicz, R. L. Taylor, and P. Nithiarasu. *The finite element method for fluid dynamics*. Elsevier/Butterworth Heinemann, Amsterdam, seventh edition, 2014.

UNIVERSITY OF DELAWARE, MATHEMATICAL SCIENCES, 501 EWING HALL, 19716
Email address: `bacuta@udel.edu`